Springer

KSME

Journal of Mechanical Science and Technology 25 (7) (2011) 1727~1735
www.springerlink.com/content/1738-494x
DOI 10.1007/s12206-011-0424-x

Effect of welding heat input on fatigue life of quenched boron steel and FB steel lap joint †

Chang Hee Suh[1], Rac Gyu Lee[1], Sang Kyun Oh[1], Yun-Chul Jung[1,*], Je-Young Son[2] and Young Suk Kim[3]

[1]*Daegu Mechatronics & Materials Institute, Daegu, 704-240, Korea*
[2]*Hwashin R&D Center, Yeongcheon, Gyeongbuk, 704-240, Korea*
[3]*School of Mechanical Engineering, Kyungpook National University, Daegu, 702-701, Korea*

(Manuscript Received May 27, 2010; Revised February 13, 2011; Accepted April 12, 2011)

Abstract

The effect of welding heat input on the fatigue life of a quenched boron steel and ferrite-bainite (FB) steel lap joint was investigated. Boron steel was quenched and welded with FB steel in heat input ranging from 0.29 to 0.67 kJ/mm. Boron, which can increase hardenability, affected the microstructure and hardness of the weld metal and heat affected zone (HAZ). The hardness of the weld metal and HAZ increased with decreasing welding heat input, and the high hardness of the weld metal and boron steel HAZ prevented the initiation of cracks in the stress concentration area around the bead. The bead width increased with increasing heat input, and the results of finite element method (FEM) showed that the maximum stress in the notch of the weld joint decreased when the bead width was increased. That is to say, the fatigue life increased when the weld joint had wider bead width. Finally, while the fatigue life was affected by the residual stress, the variation of the welding heat input used in this study had hardly any affect on the residual stress distribution.

Keywords: Boron steel; Welding heat input; Lap joint; Fatigue

1. Introduction

Boron steel is widely used in the automobile industry due to its high tensile strength above 1400 MPa after hot stamping [1]. When boron steel is used for body parts, such as bumpers, center pillars, side rails, and door beams, a high strength is only required for stiffness and crashworthiness. However, when boron steel is used for chassis parts, high fatigue life can be a more important factor than high tensile strength.

In general, the fatigue characteristics of quenched boron steel are outstanding, because the fatigue limit is known to increase with the tensile strength almost linearly [2]. In addition, since the plastic strain decreases when increasing the yield strength at a given total strain amplitude in a low cycle fatigue test, the fatigue life increases when the plastic strain energy per cycle is decreased [3, 4]. However, chassis parts are manufactured with ultra high strength steel, like quenched boron steel, and high strength steel, like ferrite-bainite (FB) steel, and assembled using gas metal arc welding (GMAW). Therefore, to apply boron steel to chassis parts, not only should the fatigue characterization of boron steel itself be considered, but so should the fatigue life of the weld joint. When steel is welded to steel, stress concentration and tensile residual stresses in the vicinity of the bead dominate the fatigue life of the weld joint, and the fatigue resistance of the weld joint generally does not increase with an increase in base metal tensile strength [5]. Therefore, the fatigue life of chassis parts is governed by the characteristics of the weld joint between quenched boron steel and dissimilar steels.

Many studies showed that the tensile residual stress and stress concentration around the bead are the major parameters affecting the fatigue life of a weld joint [6-10]. In addition, the fatigue life of a weld joint is also affected by the microstructure and strength of the weld metal and HAZ, as fatigue cracks normally initiate around the bead. When boron steel is used for weld joint, a different microstructure is formed in the weld metal and HAZ during welding when compared to a similar steel without boron. Devletian et al. [11, 12] reported that the microstructure of the weld metal and HAZ is strongly affected by the boron. During welding, boron, which can increase hardenability, transfers from the boron steel to the weld metal, thereby affecting the microstructures of the weld metal and HAZ. Moreover, the peak temperature and cooling rate which are significant parameters affecting the microstructure of the weld metal and HAZ are affected by the welding heat input.

Few studies have considered synthetically the effects of the

† This paper was recommended for publication in revised form by Associate Editor Youngseog Lee
* Corresponding author. Tel.: +82 53 608 2117, Fax.: +82 53 608 2119
E-mail address: ycjung@dmi.re.kr

Table 1. Chemical composition of base metals used in lap joint (wt%).

Materials	C	Si	Mn	P	S	Cr	Mo	Ni	B	Fe
Boron	0.24	0.22	1.19	0.01	0.002	0.14	0.001	0.007	0.002	Bal.
FB	0.08	0.09	1.52	0.02	0.002	0.01	0.002	0.008	-	Bal.

Table 2. Welding conditions used in present study.

Group no.	Current (A)	Volt (V)	Welding velocity (mm/s)	Heat input (kJ/mm)
1	160	18	10	0.29
2	220	20	10	0.44
3	230	20	10	0.46
4	240	20	10	0.48
5	240	21	10	0.50
6	240	22	10	0.53
7	280	24	10	0.67

microstructure, residual stress, and bead geometry according to welding heat input on fatigue life of the weld joint when boron steel is used. Accordingly, in this study, a lap joint, which is normally used to join chassis parts, was made by GMAW using quenched boron steel and FB590, and the effect of the welding heat input on the microstructure, bead geometry, residual stress, and fatigue life of the weld joint was investigated.

2. Experimental procedures and finite element (FE) modeling

2.1 Experimental procedures

The materials used in this study were boron steel and FB590 (512 MPa yield strength and 605 MPa tensile strength), and the chemical compositions are presented in Table 1. Boron steel consists of ferrite and perlite, while FB590 consists of ferrite and bainite. The boron steel and FB590 were 2.8 mm and 4 mm thick, respectively, and cut into 250 mm × 250 mm plates. As boron steel is normally used after hot stamping, the plates of boron steel were austenitized for 7 minutes at 930℃, and then quenched with water to simulate hot stamping. The quenched boron steel, which included martensite, had a tensile strength of 1551 MPa and yield strength of 1230 MPa.

The plates were fixed to a welding jig and a lap joint welded using GMAW. The shielding gas consisted of Ar 80% - CO2 20%, the welding wire was AWS A 5.18 ER70S-G (Fe - 0.07C - 0.84Si - 1.95Mn - 0.31Mo - 0.17Ti) with a 1.2 mm diameter, and the expected hardness of the weld metal was about 200 Hv after welding. The welding heat input was used as the main parameter in this study, and the welding conditions are shown in Table 2.

The surface of the specimen was mechanically polished and etched, and the microstructure was then analyzed using an optical microscope (OM). A hardness test of the HAZ and weld metal 1mm below the surface was carried out at 4.9 N using a Vickers hardness tester (Tukon 2100). For the tensile and fatigue specimens, the welded plates were cut by wire electrical discharge machining (WEDM), and then machined carefully using an NC machine to eliminate the HAZ created by the WEDM. The final shape of the specimens is shown in Fig. 1. All the tensile tests were performed at a constant velocity of 1.67×10^{-2} mm/s (1 mm/min) using a displacement controlled mode, while an extensometer was used to measure the elongation accurately. The engineering stress based on an initial cross-section of the boron steel was used to investigate the mechanical behavior of the weld joint, and 0.2% offset yield strength was used. All the fatigue tests were conducted at 10 Hz, and the stress ratio was 0.1. All the specimens for the tensile and fatigue tests were prepared as per KS B 0801 No.5, and the tensile and fatigue tests carried out using 100 kN servo hydraulic machine (MTS 810). A residual stress tester (XSTRESS3000) was used to evaluate the residual stress along the welding line direction and transverse direction in the HAZ area.

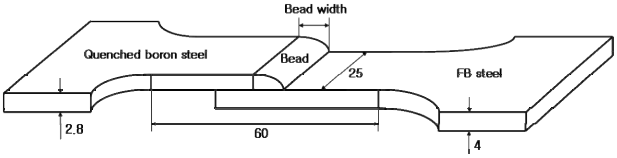

Fig. 1. Welded specimen for tensile and fatigue tests (unit: mm).

2.2 FE modeling

One of main parameters determining the fatigue life of a weld joint is the weld bead geometry. Thus, since the fatigue life of a weld joint is affected by a combination of the microstructure, hardness, residual stress, and bead geometry, a finite element method (FEM) was adopted to investigate just the effect of the bead geometry. As the bead width varies with the welding heat input, a simulation was performed to evaluate the stress concentration resulting from the variation of the bead width. The bead width used in the simulation was selected by a cross-section observation of the weld joint. The bead geometries used in the FEM are shown in Fig. 2 and Table 3. The simulation assumed a plane strain condition. The size of the specimen made using the finite element model was 60 mm and the size of the element was about 0.1 mm, which was enough to express the stress concentration. One end of the finite element model was fixed and the load used for the fatigue test was applied to another end, then an elastic simulation was performed. Young's modulus and Poisson's ratio for both the boron steel and the FB590 was 210 GPa and 0.3, respectively, and finite element code MARC 2008 was used.

Table 3. Bead geometry used in FE model.

Bead geometry no.	Bead width (mm)	Radius of bead toe (mm)
1	4.5	0.5
2	5.5	
3	6.5	
4	7.5	

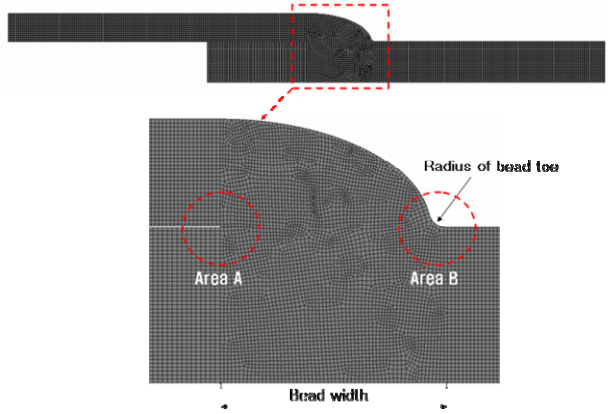

Fig. 2. FE model of plane strain condition for weld joint.

3. Results

3.1 Microstructure and bead geometry

In a lap joint, since fatigue cracks normally initiate around the bead, the microstructures of both the weld metal and the HAZ are important. The aspect of the microstructure distribution remained similar, regardless of the welding heat input, as shown by the representative aspect for Group 4 in Fig. 3. The lap joint consisted of six HAZ areas and the weld metal area after welding. The boron steel HAZ was divided into HAZ1(Boron), HAZ2(Boron), and HAZ3(Boron), while the FB590 HAZ was divided into HAZ1(FB), HAZ2(FB), and HAZ3(FB). HAZ1(FB) and HAZ2(FB) coexisted around the bead toe area.

The microstructures of the weld metal according to the welding heat input are shown in Fig. 4. Martensite was observed in Group 1 due to the low welding heat input, whereas acicular ferrite and martensite were observed in Groups 2~7, and the amount of acicular ferrite became larger when increasing the welding heat input. In Groups 1~7, the aspect of the microstructure distribution in the HAZ remained almost the same, regardless of the welding heat input, as represented by the microstructure for Group 4 shown in Fig. 5. In Fig. 5(a), HAZ1(Boron) was austenitized above A3 and then rapidly cooled, resulting in the formation of martensite. In. Fig. 5(b), the temperature at HAZ2(Boron) was elevated above A1 and then cooled, resulting in the formation of multiple phases of martensite, bainite, and ferrite. In Fig. 5(c), the temperature at HAZ3(Boron) was elevated below A1 and then cooled, thereby tempering the martensite formed from the water

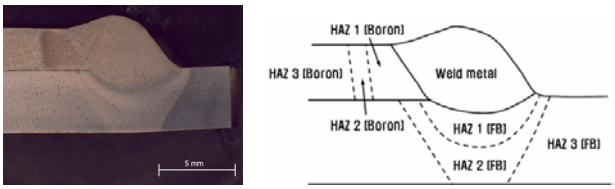

Fig. 3. Real and schematic cross-section view of welded specimen from Group 4 (0.48 kJ/mm).

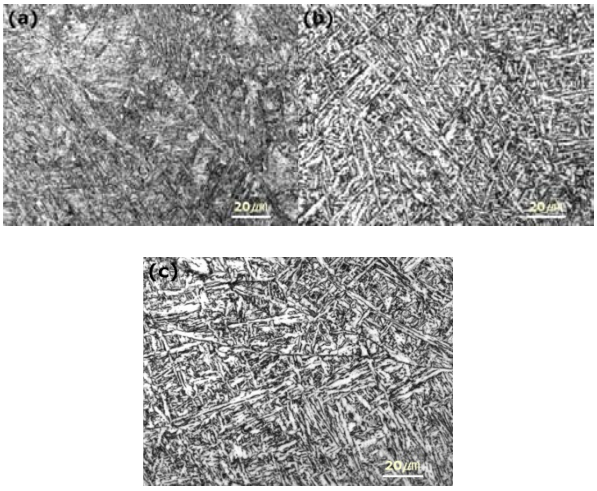

Fig. 4. Optical microstructures of weld metal : (a) Group 1 (0.29 kJ/mm); (b) Group 4 (0.48 kJ/mm); (c) Group 7 (0.67 kJ/mm).

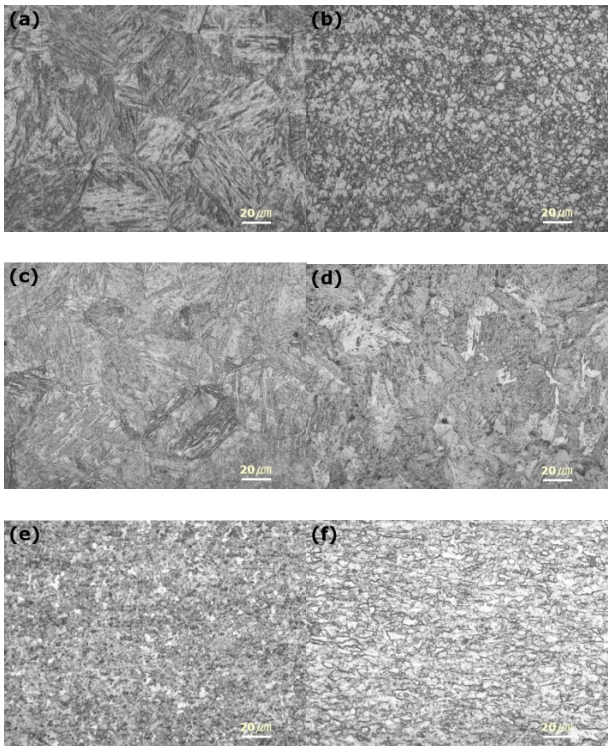

Fig. 5. Optical microstructures of HAZ : (a) HAZ1(Boron); (b) HAZ2(Boron); (c) HAZ3(Boron); (d) HAZ1(FB); (e) HAZ2(FB); (f) HAZ3(FB).

Table 4. Cross-sectional geometries of bead.

Group no.	Weld penetration (mm)	Bead width (mm)	Bead toe radius (mm)
1	0.3	4.1	0.5
2	0.9	5.5	0.7
3	1.2	5.8	1.0
4	1.3	5.8	1.0
5	1.3	5.8	0.5
6	1.3	6.5	0.8
7	2.0	8.5	0.8

quenching. In Fig. 5(d), HAZ1(FB) was austenitized above A3 and then rapidly cooled, resulting in the formation of martensite and bainitic ferrite. In. Fig. 5(e), the temperature at HAZ2(FB) was elevated above A1 and then cooled, resulting in the formation of multiple phases of non transformed ferrite-bainite and transformed ferrite.

In Fig. 5(f), the temperature at HAZ3(FB) was elevated below A1 and then cooled, resulting in the formation of heat-affected ferrite and bainite.

The results of cross-sectional observation are shown in Table 4. The bead width increased with the welding heat input. However, all the bead toe radii were within a range of 0.5~1.0, and unaffected by the welding heat input. The weld penetration, which is the most important parameter for evaluating the welding reliability, increased with the welding heat input and was good (0.9~1.3 mm) for Groups 2~6, too shallow (0.3mm) for Group 1, and too deep (2 mm) for Group 7.

3.2 Tensile strength and hardness

In the tensile tests, all the cracks initiated in area A with the maximum stress concentration, and propagated along the boundary between the weld metal and HAZ1(Boron). Multiple stresses, including tensile and shear stresses, were generated in the lap joint during the tensile tests, as the axes of loading did not correspond. As the stress and strain were relatively higher in area A than in area B, all the cracks were initiated in area A. Although the tensile tests were not performed in a uniform tensile mode, the results were useful to evaluate the relative bonding strength of the lap joint. Additionally, the initial cross-section area of the boron steel was used to calculate the engineering stress of the lap joint.

The results of the tensile test are shown in Fig. 6. The tensile strength for Group 1 was slightly high, and this strength gradually increased from Group 2 to Group 7. Martensite, which has a high strength, affected the tensile strength of the lap joint in Group 1 in spite of a shallow weld penetration. In Groups 2~7, it was expected that the tensile strength would be decreased, due to the increased amount of acicular ferrite and the decreased volume fraction of martensite with a higher

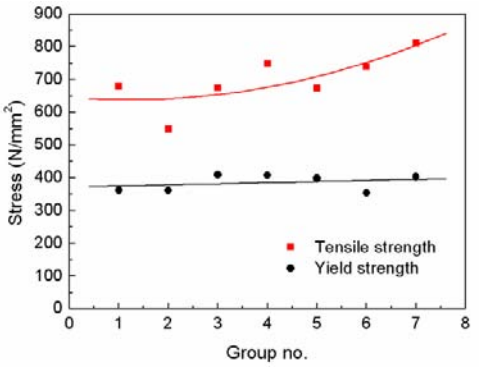

Fig. 6. Tensile test results for welded specimens.

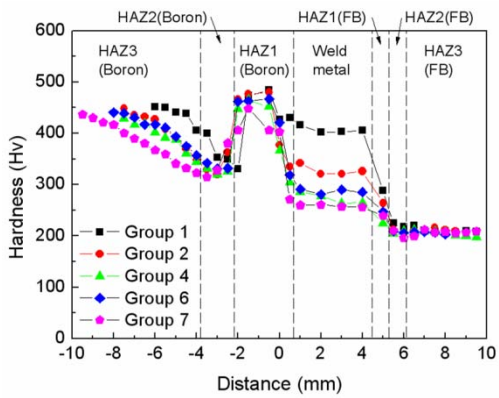

Fig. 7. Hardness test results for weld metal and HAZ.

welding heat input. However, the tensile strength increased in the real test, as the resistance to deformation increased with the weld penetration and bead width.

The results of the hardness tests are shown in Fig. 7. The hardness of the weld metal decreased when increasing the welding heat input for Groups 2~7, which was expected based on the microstructure observation. Plus, the maximum hardness of the boron steel HAZ and FB590 HAZ decreased when increasing the welding heat input. This was because the high cooling rate and low peak temperature with a low welding heat input resulted in the formation of fine grains and suppressed the tempering effect.

The hardness at HAZ1(Boron) was higher than the hardness at HAZ1(FB) due to the hardenability effect of boron and solid solution strengthening by the carbon contained in the boron steel. As fatigue cracks normally initiate around the bead, especially at the notch in area A, a higher hardness for the weld metal and HAZ1(Boron) can prevent the initiation of fatigue cracks. As the hardness at the bead toe radius in the FB590 was low (about 200 Hv), the fatigue life of the lap joint would be decreased if a stress concentration occurred and fatigue cracks were initiated in this area.

3.3 Residual stress

The residual stress measurements were performed using

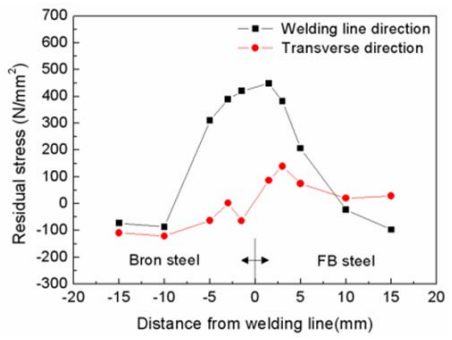

(a)

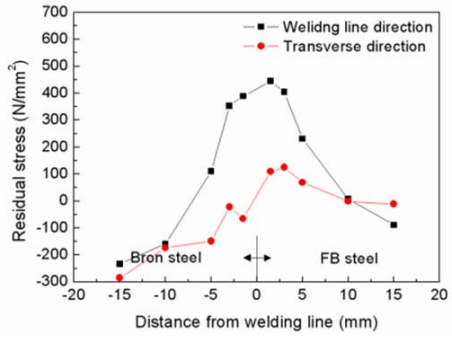

(b)

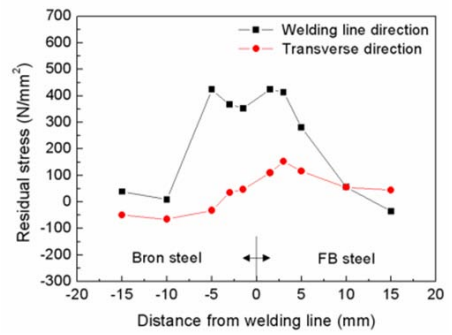

(c)

Fig. 8. Residual stress distribution for welded specimens (a) Group 2 (0.44 kJ/mm); (b) Group 4 (0.48 kJ/mm); (c) Group 6 (0.53 kJ/mm).

Groups 2, 4, and 6, which had a good weld penetration, and the results are shown in Fig. 8. The distribution of residual stress was almost the same in all three Groups. The peak tensile residual stress along the welding line direction was generated at HAZ1 in all three Groups, and the magnitude decreased when leaving the weld line. The difference between Fig. 8(a), (b) and (c) near the weld line was considered a measurement error. The residual stress along the transverse direction was shown as a symmetrical shape, so the dissimilar steels did not affect the distribution of residual stress. However, the tensile residual stress along the transverse direction at HAZ1(FB) was higher than that at HAZ1(Boron). As a high tensile residual stress at HAZ1(FB) can promote crack initiation, it is expected that fatigue life of the lap joint would be decreased if fatigue cracks were initiated in this area.

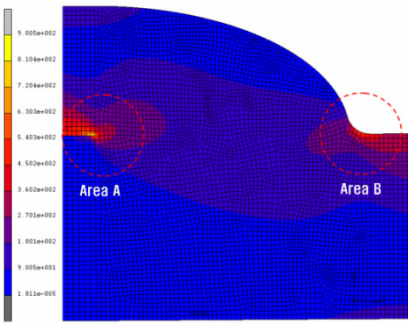

Fig. 9. Effective stress distribution of Bead geometry no. 2 (5.5 mm bead width and 0.5 mm bead toe radius specimen).

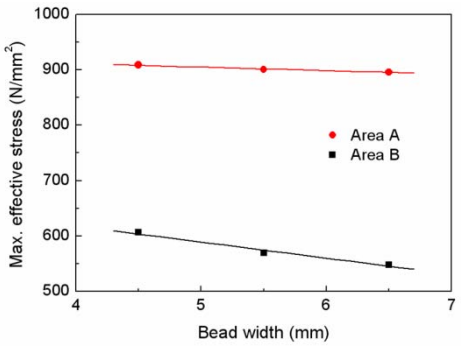

Fig. 10. Maximum effective stress for 0.5 mm bead toe radius specimen according to bead width, when the applied load was 9.8 kN.

It has been reported that tensile residual stress is increased when increasing the welding heat input [13], however, the distribution and magnitude of residual stress remained almost the same, as the variation in the welding heat input used in this study was not significant.

3.4 Finite element analysis

The stress concentration changes with the bead geometry, which in turn varies according to the welding heat input. However, as the variation of the bead toe radius with the welding heat input was minimal, it was assumed that the bead toe remained the same and only the effect of the bead width on the stress concentration was investigated by FEM. The boundary condition was the bead geometry no. 2 (bead width of 5.5 mm and bead toe radius of 0.5 mm) and the applied load was 9.8 kN (the maximum load in a plane strain condition when the fatigue test was performed under 8.820 kN). The results of the simulation are shown in Fig. 9.

When comparing the stress concentration in areas A and B, the maximum stress in area A was approximately 1.5 times higher than that in area B. The variation of the effective stress with the bead width when the applied load was 9.8 kN is shown in Fig. 10. While the maximum stress in areas A and B decreased when increasing the bead width, the rate of decrease in area B was higher than that in area A. Conversely, while the maximum stresses in areas A and B decreased when decreasing the applied load in case of bead geometry no. 2, the rate of

Table 5. Fatigue test results for Groups 2 (0.44 kJ/mm) and 6 (0.53 kJ/mm).

Load range (kN)	Group 2		Group 6	
	Fatigue life (cycles)	Fracture location	Fatigue life (cycles)	Fracture location
9.702	137,055	Area B	23,629	Area A
8.820	137,853	Area B	46,579	Area A
7.938	164,587	Area B	195,118	Area B
7.056	228,667	Area B	301,571	Area B
6.174	428,393	Area B	1,063,498	Area B

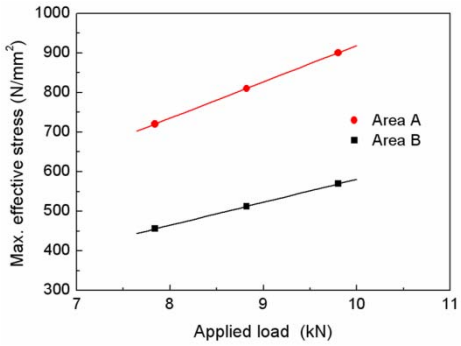

Fig. 11. Maximum effective stress of Bead geometry no. 2 (5.5 mm bead width and 0.5 mm bead toe radius specimen) according to applied load.

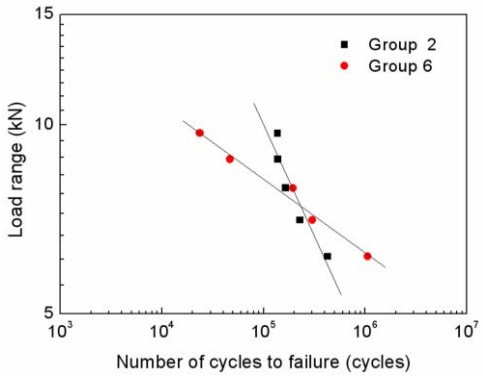

Fig. 12. The comparison of fatigue life between Groups 2 (0.44 kJ/mm) and 6 (0.53 kJ/mm) according to load range.

decrease in area A was higher than that in area B (Fig. 11).

3.5 Fatigue life

The fatigue test was performed using specimens from Groups 2 and 6, which had good weld penetration, and the results are shown in Fig. 12 and Table 5. Fatigue fractures occurred in area B in all the specimens from Group 2. However, for the specimens from Group 6, fatigue fractures occurred in area A in the case of a high applied load over 8.820 kN, whereas fatigue fractures occurred in area B in the case of a low applied load below 8.820 kN. The fatigue life of the lap joint was remarkably low when the fatigue fractures occurred in area A. The fatigue life of the specimens from Group 6, which were made with a high welding heat input, was higher than that of the specimens from Group 2 when a fatigue fracture occurred in area B.

Table 6. Microstructures of B-free and B-added steels according to cooling rate.

Cooling rate	B-free steel	B-added steel
Low	Primary ferrite Widmanstätten ferrite	Primary ferrite (small) Accicular ferrite Martensite (small)
High	Primary ferrite Widmanstätten ferrite Bainite Martensite	Martensite (almost)

4. Discussion

4.1 Effect of microstructure and hardness on fatigue life

In this study, fatigue fractures were generated in all groups at the boundary between the weld metal and HAZ1, and the microstructure, hardness, and residual stress of the weld metal and HAZ were changed by the welding heat input. Acicular ferrite and martensite were both generated in the cases of Group 2 (0.44 kJ/mm) and Group 6 (0.53 kJ/mm). The amount of acicular ferrite increased and the volume fraction of martensite decreased when increasing the welding heat input. Yet, the fatigue life of the specimens in Group 6 increased under an applied load of 7.938 kN.

It has already been reported that the formation of acicular ferrite is controlled by the welding heat input, and if the welding heat input is higher, the content of acicular ferrite will be lower. However, the welding heat input used in this study was low, so acicular ferrite was formed in most groups. Plus, the presence of acicular ferrite in the weld metal is usually assumed to be good for strength and toughness when compared with other types of ferrite (pro-eutectoid ferrite or polygonal ferrite), and the fine grain size of acicular ferrite provides a high resistance to fatigue crack propagation [14, 15]. Yet, in this study, the fatigue life increased with an increase in the acicular ferrite grain size, implying that the residual stress and bead geometry had a much higher effect on the fatigue life than the microstructure of the weld metal.

The microstructure of the weld metal is affected by the boron content and cooling rate. The effect of the cooling rate is shown in Table 6, and the optimal boron content is 0.0015~0.003% to increase the hardenability effect [11, 12]. In this study, the boron content was about 0.002%. Also, martensite is formed in boron steel with a high cooling rate and acicular ferrite formed with a low cooling rate. The results from the study by Devletian et al. agreed with the results of this study, as martensite was formed in Group 1, while acicular ferrite was formed in Groups 2~7. Although the welding

wire used in this study did not include boron, the microstructure of the weld metal was similar to a microstructure of boron including the welding wire, indicating that boron had been transferred from the boron steel to the weld metal.

HAZ1(Boron) was austenitized due to the welding heat input, and rapidly cooled in the atmosphere resulting in the formation of matensite. HAZ1(FB) underwent a similar temperature history, resulting in a multiple phase of bainitic ferrite and martensite. Martensite was formed at HAZ1(Boron), as the hardenability was increased and the martensite start temperature (Ms) was lower due to the boron, whereas bainitic ferrite and martensite were formed at HAZ1(FB), as there was no boron at that area. In addition, the amount of carbon, which increases the solid solution strengthening, was about three times higher in the boron steel than in the FB590.

As shown in the hardness test, the hardness at HAZ1(Boron) was about 400 Hv, while the hardness at HAZ1(FB) was 200~250 Hv. Thus, it would appear that the martensite at HAZ1(Boron) increased the fatigue life of the weld joint.

In the fatigue test under an applied load of 7.938 kN, the fatigue fractures were all generated in area B, instead of area A with the highest stress concentration. This was because the martensite and high hardness at HAZ1(Boron) suppressed the initiation of fatigue cracks in area A. Meanwhile, in the fatigue test under an applied load of 7.938 kN, the fatigue life of Group 6 was superior to that of Group 2, which was contrary to expectations, as it was anticipated that the fatigue life of Group 6 (low cooling rate) would be lower than that of Group 2 (high cooling rate) due to the increased bainitic ferrite and decreased hardness. However, the real test results implied that the fatigue life of the lap joint was more affected by stress concentration due to the bead geometry than the microstructure and hardness when fatigue cracks occurred in area B. That is to say, if fatigue fractures occur in area B, controlling the bead geometry is the most effective way to increase the fatigue life of the lap joint.

In the fatigue test with an applied load over 8.820 kN, fatigue fractures were generated in area A in the case of Group 6 and in area B in the case of Group 2. As shown in Fig. 10, the hardness and microstructure at HAZ1(Boron) decreased when increasing the welding heat input, although the maximum effective stress in area A was hardly affected by the bead width. Thus, the fatigue cracks were initiated in area A in the case of a high welding heat input. In Fig. 11, the maximum effective stress in area A increased rapidly when increasing the applied load compared to that in area B, which led to local plastic deformation at the notch in area A. As a result, fatigue cracks were initiated at the boundary between the weld metal and HAZ1(Boron).

Plus, since the fracture toughness of the martensite generated by the water quenching was low, when fatigue cracks were initiated, the cracks rapidly propagated to a final fracture. Thus, the fatigue life of the weld joint was decreased. Therefore, since quenched boron steel after a hot stamping process is normally used without tempering, the welding line should be designed to avoid a stress concentration in area A.

4.2 Effect of residual stress and bead geometry on fatigue life

Residual stress is one of the main parameters affecting the fatigue life of a lap joint. It has already been reported that the fatigue life is decreased when increasing the tensile residual stress, yet increased when increasing the compressive residual stress [16, 17]. The residual stress after welding was affected by the welding heat input, and the variation of the welding heat input affected the cooling rate at the weld metal and HAZ. Thus, the microstructure and mechanical properties of the weld metal and HAZ were changed [18].

In this study, in the case of Groups 2~6 with a good weld penetration, the maximum tensile residual stress was generated along the welding line direction at HAZ1. Plus, the distribution of the residual stress according to the welding heat input was almost the same. However, the tensile residual stress along the transverse direction was a little high at HAZ1(FB) when compared to that at HAZ1(Boron).

It has been reported that materials expand and shrink during welding and cooling, resulting in the generation of residual stress [13]. However, in this study, since there was no significant change in the level and distribution of residual stress, this implies that the range of the welding heat input used was not high enough to affect level and distribution of residual stress.

The residual stress generated after welding is considered one of the main factors affecting the fatigue life of a lap joint. However, in this study, since the residual stress was not significantly affected by the variation of the welding heat input, it would appear that the fatigue life of the lap joint was mainly affected by the bead geometry, microstructure, and hardness. Nonetheless, the higher tensile residual stress at HAZ1(FB) than at HAZ1(Boron) may have moved the crack initiation point to HAZ1(FB), thereby decreasing the fatigue life of the weld joint. When welding dissimilar materials, like stainless steel and carbon steel, the residual stress distribution is not symmetric based on the weld line [13]. Yet, the residual stress distribution was symmetric after welding the boron steel and FB steel, implying that the added boron in the boron steel did not affect the residual stress.

Bead geometry is also a major factor affecting the fatigue life of a weld joint, similar to residual stress, as the stress concentration is affected by the bead geometry. As shown in Fig. 9, the stress was concentrated in areas A and B when an external load was applied to the lap-jointed fatigue specimen. Plus, the maximum stress in area A was 1.5 times higher than that in area B. Thus, if the lap joint has the same microstructure, hardness, and residual stress, the possibility of fatigue crack initiation of the weld joint would be expected to be higher in area A than in area B due to the higher stress concentration in area A. However, in most fatigue tests, the fatigue fractures were generated in area B, as the microstructure and hardness

in area A were superior to those in area B, thereby improving the fatigue life. The microstructures around the notch in area A, where the fatigue cracks were initiated, were the boundary of the martensite at HAZ1(Boron) and the acicular ferrite in the weld metal, and the minimum hardness of the boundary was about 320 Hv. In contrast, the microstructures around the notch in area B were multiple phases of bainitic ferrite and martensite at HAZ1(FB), multiple phases of ferrite and bainite at HAZ2(FB), and acicular ferrite in the weld metal. The minimum hardness between HAZ1(FB) and HAZ2(FB), where the fatigue cracks were initiated, was about 200 Hv. Therefore, the microstructure and hardness had a higher effect on the fatigue life than the stress concentration, meaning that most of the fatigue fractures occurred in area B.

In the fatigue test under an applied load of 7.938 kN, all the fatigue fractures occurred in area B, and the fatigue life of Group 6 with a high welding heat input was superior to that of Group 2. Many researchers have reported that the fatigue life of a weld joint is increased when increasing the bead toe radius due to a reduced stress concentration [6-8]. However, in this study, there was no clear relationship between the bead toe radius and the welding heat input, although the bead width increased when increasing the welding heat input. As shown in Fig. 9, when the lap joint maintained the same bead toe radius, the maximum stress in area B was decreased when increasing the bead width. In the fatigue test under an applied load of 7.938 kN, in spite of the low hardness in area B caused by the high welding heat input, the expanded bead width decreased the stress concentration, thereby increasing the fatigue life of the lap joint. The results in Fig. 6, where the tensile strength increased when increasing the welding heat input, except in the case of Group 1, support this circumstance. That is to say, the expanded bead width increased the deformation resistance, thereby increasing the tensile strength. Thus, it would appear that the effect of the bead geometry on the strength and fatigue life was as high as the effect of the microstructure and hardness.

In the fatigue test under an applied load over 8.820 kN, fatigue fractures occurred in area A. As shown in Fig. 11, the higher the applied load, the higher the stress increase in area A, resulting in plastic deformation at the notch in area A, as the ductility and fracture toughness of the notch in area A were inferior due to the microstructure of the boundary between HAZ1(Boron) and the weld metal. Furthermore, since the maximum stress in area A was higher than that in area B, the propagation life was decreased when fatigue cracks were initiated in area A. Thus, the total fatigue life was decreased.

5. Conclusions

The effect of the welding heat input on the fatigue life of a boron steel and FB steel lap joint was studied and the following results obtained:

(1) In a lap joint of boron steel and FB steel, the fatigue life was increased when increasing the welding heat input and the fatigue cracks were initiated at the bead toe radius of the FB steel, whereas the fatigue life was decreased under a high applied load when the fatigue fractures occurred at the notch in area A.

(2) Acicular ferrite and martensite were formed in the weld metal due to the diffusion of boron from the boron steel into the weld metal part, thereby increasing the fatigue life of the lap joint.

(3) After welding, martensite was formed throughout HAZ1(Boron), due to the increased hardenability effect of boron. The high hardness of the martensite at HAZ1(Boron) then suppressed the initiation of fatigue cracks and increased the fatigue life of the lap joint.

(4) The maximum tensile residual stress occurred in HAZ1, and the distribution and level did not change according to the welding heat input. Thus, it would appear that the variation in the welding heat input used in this study was not high enough.

(5) The results of FEM showed that the maximum stress was generated in the notch (areas A and B) of the weld joint and the value was affected by bead width, which changed according to welding heat input. An increase in bead width reduces the stress concentration of the weld joint notch.

(6) As fatigue fractures occurred at the bead toe radius in the lap joint when the applied load was low, increasing the bead toe radius and bead width is recommended to improve fatigue life. Additionaly, the welding line should be well designed to reduce the maximum stress at the notch in area A. The propagation life was very short when fatigue cracks were initiated in area A, resulting in a sudden fracture.

References

[1] M. S. Chae, G. D. Lee, Y. S. Suh, K. H. Lee and Y. S. Kim, Mechanical and forming characteristics of high-strength boron-alloyed steel with hot forming, *Trans. Mater. Process*, 18 (3) (2008) 236-244.

[2] J. A. Bannantine, J. J. Comer and J. L. Handrock, Fundamentals of metal fatigue analysis, Prentice Hall, New Jersey, USA (1990) 1-30.

[3] A. M. Sherman and R. G. Davies, The effect of martensite content on the fatigue of a dual phase steel, *Int. J. Fatigue* January (1981) 36-40.

[4] P. C. Chakraborti and M. K. Mitra, Room temperature low cycle fatigue behavior of two high strength lamellar duplex ferrite martensite (DFM) steels, *Int. J. Fatigue,* 27 (2005) 511-518.

[5] Society of automoive engineer, SAE fatigue design handbook, 3rd Edition, SAE International, Pennsylvania, USA (1997) 92-97.

[6] T. N. Nguyen and M. A. Wahab, The effect of weld geometry and residual stresses on the fatigue of welded joints under combined loading, *J. Mater. Process. Technol*., 77 (1998) 201-208.

[7] T. L. Teng, C. P. Fung and P. H. Chang, Effect of weld geometry and residual stresses on fatigue in butt welded joints, *Int. J. Press. Vessels Piping,* 79 (2002) 467-482.

[8] B. Goo, J. Kim, J. Seo and C. Seok, A study on the effect of welding residual stress and weld bead profiles on fatigue be-

havior, *Key Eng. Mat*., 270 - 273 (2004) 2302-2307.
[9] T. L. Teng and P. H. Chang, Effect of residual stresses on fatigue crack initiation life for butt welded joints, *J. Mater. Process. Technol*., 145 (2004) 325-335.
[10] T. L. Teng and C. C. Lin, Effect of welding conditions on residual stresses due to butt welds, *Int. J. Press. Vessels Piping,* 75 (1998) 857-864.
[11] J. H. Devletian, Borocarbide precipitation in the HAZ of boron steel welds, *Welding J*., 55 (1) (1976) 5-12.
[12] J. H. Devletian and R. W. Heine, Effect of boron content on carbon steel welds, *Welding J*., 54 (2) (1975) 45-53.
[13] D. Akbari and I. Sattari-Far, Effect of the welding heat input on residual stresses in butt welds of dissimilar pipe joints, *Int. J. Press. Vessels Piping,* 86 (2009) 769-776.
[14] F. J. Barbaro and P. Krauklis, K. E., Formation of acicular ferrite at oxide particles in steels, *Mater. Sci. Technol*., 5 (1989) 1057-1068.
[15] B. Dixon and K. Hakansson, Effect of welding parameters on weld zone toughness and hardness in 690 MPa steel, *Welding J*., 74 (4) (2002) 122-132.
[16] D. V. Nelson, Effect of residual stress on fatigue crack propagation, residual stress effects in fatigue, *ASTM STP,* 776 (1982) 172-174.
[17] K. Chongmin and D. E. Diesburg, Effect of residual stress on fatigue fracture of case hardened steels - an analytical model, residual stress effects in fatigue, *ASTM STP,* 776 (1982) 224-234.
[18] P. H. Chang and T. L. Teng, Numerical and experimental investigations on the residual stresses of the butt welded joints, *Computational Mater. Sci*., 29 (4) (2004) 511-522.

Chang Hee Suh received his B.S. and M.S. degrees in Mechanical Engineering from Kyungpook National University, Korea, in 1998 and 2001. He is a senior researcher at the Daegu Mechatronics & Materials Institute. His research interests include computational mechanics, material processing, and fracture mechanics.

Young Suk Kim is currently a professor, Department of Mechanical Engineering, Kyungpook National University in Daegu, Korea. He received his B.S. degree from Hanyang University in 1979 and M.S. degree from Seoul National University in 1981. He received his Ph.D degree from Kobe University, Japan, in 1986. Dr. Kim's research interests include sustainable material processing, nano/micro mechanics, FEM and biomechanics.

Yun-Chul Jung received his B.S. degree from Donga University, Korea, in 1991. He received his M.S. and Ph.D degrees from Ehime University, Japan, in 1994 and 1997. He is a principal researcher at the Daegu Mechatronics & Materials Institute. His research interests include control of microstructure, analysis of nano structure, and analysis of atomic structure.